

Analysis of Electrochemical Impedance and Noise Data for AISI-310 Exposed to Lithium Bromide Solution

C. Cuevas-Arteaga*, M. Luna Brito, A. Molina-Ocampo, J. Colín, S. Serna-Barquera, A. Torres-Islas.

Centro de Investigación en Ingeniería y Ciencias Aplicadas-Facultad de Ciencias Químicas e Ingeniería, Universidad Autónoma del Estado de Morelos. Av. Universidad 1001, Col. Chamilpa, Cuernavaca, Morelos, C.P. 62209, México.

*E-mail: ccuevas@uaem.mx

Received: 10 May 2013 / Accepted: 14 June 2013 / Published: 1 July 2013

The corrosion behavior of AISI-310 in aqueous lithium bromide solution (50.0 % w/w) at 25, 60 and 80°C has been studied through polarization curves (PC), the electrochemical noise technique (EN) and the electrochemical-impedance spectroscopy (EIS). Physical characterization of the corroded samples indicated that AISI-310 exposed at 25°C suffered a uniform corrosion process, whereas at 60 and 80°C a mixed corrosion process was observed, which was in agreement with the localization indexes calculated from EN data. The corrosion activity was analyzed taking into account the noise pattern, which was alike for the three test temperatures, observing a low amplitude/high frequency noise with some medium intensity current transients, especially at the highest temperature. EIS results showed that the temperature is an important issue in the corrosion controlled reaction, since at 25°C, a pure diffusion-controlled reaction was predominantly seen, at 60°C an activation-controlled step was observed, whereas at the higher temperature both diffusion and charge transfer controlled steps were observed. The corrosion kinetics was calculated from the resistance noise obtained from EN data, and then the Stern-Geary equation and the Faraday's Law were used. The corrosion kinetics showed that at 60°C the corrosion rate was somewhat higher than that at 80°C, which could also be seen in the electrochemical current noise, where the current density was higher at 60°C. This behavior was supported due to the changes in the thermodynamic characteristics of the lithium bromide solution, since at 80°C the aqueous solution at the experimental concentration tends to crystallize.

Keywords: Stainless steel, electrochemical noise, lithium bromide, heat pumps

1. INTRODUCTION

Some of the most interesting heat exchanger-recovery systems are the absorption heat pump/transformers, which utilize waste heat energy to transform it in useful energy in an

environmental friendly way. In general, it could be said that the heat pumps are capable to increase the temperature from an intermediate temperature heat resources to a 50.0% higher, while the rest is dissipated to the environmental [1,2]. These devices use a mixture solution of two chemical substances called working fluid and absorbent. One of the common mixtures used in heat pumps is a 50.0% w/w LiBr absorbent/water solution (working fluid), which under system operating conditions has been reported as highly corrosive for stainless steels, making it necessary to use corrosion inhibitors [3-5]. Several attempts have been made to determine the corrosion resistance of numerous materials including the stainless steels exposed to LiBr-H₂O solutions to the application to heat pumps, nevertheless until now there are no materials which have a good performance under lithium bromide aqueous solutions conditions and the corrosion mechanisms about this systems are not comprehended at all. In these works, the studied materials have been some stainless steels as 304, 316, 316L, 174, 430, some carbon steels as G4135, G10450 and G10150, and the alloy 33 and titanium [3,4]; some stainless steel UNS-N08031 (iron base) an UNS-N06059 (nickel base) under welded and non-welded conditions [5]; some duplex stainless steels as EN-14311, 14429 and 14462 [6,7]. These studies have been performed under different concentrations of LiBr in a range of temperatures of 25-80°C, applying the conventional weight loss method, polarization curves, an open circuit potential measurements. The application of the Tafel extrapolation method to obtain *i*_{corr} (corrosion current density) and *E*_{corr} (corrosion potential) has been also presented. The results showed that all the materials are susceptible to be degraded in a general or localized corrosion, being the AISI-316 more resistant than the AISI-304. From that reports, chromium has conferred the major corrosion resistant to the materials forming the Cr₂O₃ as the passive oxide. Some other works have been published presenting the study of several stainless steels with different composition in chromium such as AISI-304 [8,10], AISI-304L [3,11], AISI-316 [12], and AISI-316L [13], where polarization curves, the electrochemical noise technique (EN) and the conventional weight loss method were used. In these works the corrosion kinetics during 15 days obtained from the EN technique were presented together with the SEM analyses, observing an important effect of the composition in chromium on the corrosion rate. All these alloys were susceptible to corrode in a localized corrosion. From the works above cited, it is possible to say that until now there are no materials totally resistant to LiBr solutions at temperatures below 80°C, being necessary to study some other materials particularly with a high concentration of chromium, since as it has said before, this element seems to be one of the most corrosive resistant in this aqueous media. That is why the aim of the present work was to evaluate the corrosion resistance of another stainless steel with a major composition of chromium (24-26%) and nickel (19-22%) with respect to AISI-304, AISI-304L, AISI-316 and AISI-316L. In addition, in the particular case of AISI-310, this also contains 1.5% of silicon, with which, it is expected to obtain better results under the LiBr aqueous solution. This study reports a corrosion evaluation of AISI-310 exposing to 50.0 % w/w BrLi-H₂O at low temperatures using the electrochemical noise technique to obtain the kinetics corrosion during 10 days, the electrochemical impedance spectroscopy to determine some characteristics of the controlled reaction, and the potentiodynamic polarization curves, through which some corrosive parameter will be determined to elucidate some corrosion mechanisms.

2. EXPERIMENTAL PROCEDURE

The corrosive solution was prepared with lithium bromide analytical grade reagents and distilled water (50.0 % w/w). Each experiment was made utilizing 100 ml of corrosive solution, which was placed in an open flask, and then the flask was placed on an electrical heater to obtain the test temperatures at 60 and 80°C. The electrodes were made of a commercial sheet of stainless steel AISI-310, whose composition was (wt %): 25.0Cr-21.5Ni-1.5Si-2.0Mn-0.25maxC-49.75Fe. The samples for the electrochemical techniques were cut to size 10.0 x 5.0 x 2.0 mm, and then were grounded to 600 grit silicon carbide paper, rinsed with distilled water, degreased with acetone and dried under a warm air stream. For electrical connection, the specimens were spot welded to an 80.0Cr-20.0Ni wire, 150 mm long and 1 mm in diameter, and then the wire was isolated from the corrosive solution introducing it inside glass tubes; the gap between the glass tube and electrical connection wire was filled with refractory silicon. The polarization curves were carried out applying an over-potential of -400.0 mV below to 800.0 mV above the corrosion potential at a sweep rate of 1.0 mV/s [6,7]. The electrochemical cell included the stainless steel AISI-310 working electrode, an Ag/AgCl electrode as a reference electrode and a platinum wire as the auxiliary electrode.

Electrochemical potential and current noise measurements were obtained using a three 'identical' electrodes set-up, recording 1 reading/s to produce records of 1024 points every 4 hours during 10 days. EIS measurements were performed between 0.1 to 10000 Hz, and the amplitude of the input sine-wave voltage was 10 mV. Several impedance diagrams were obtained continuously for 24.0 hours. The three electrochemical methods were performed using an ACM Gill 8AC potentiostat controlled by a personal computer.

Scanning electron microscopy (SEM) coupled with energy dispersive X-ray analysis (EDAX) was used to study the surface morphology of the corroded specimens and for determining qualitative analyses. SEM analysis was carried out through the Zeiss DSM 960 microscopy.

3. RESULTS AND DISCUSSION

3.1. Physical Corrosion Characterization

Figure 1 shows three SEM images of the working electrode performing as the anode of the electrochemical cell when applying EN after exposure at 25, 60 and 80°C respectively, together with the images are also presented EDX analysis of the corrosion products presented in the corresponding image. EDX analysis at 60 and 80°C were taken from the inside of pits.

These images were selected for evidencing the existence of localized and/or general corrosion activity presented in the corroded samples. Figure 1.a presents an apparent uniform corroded surface with many corrosion products over the surface; the marks of the polish process are not seen, which means that a generalized corrosion process was carried out.

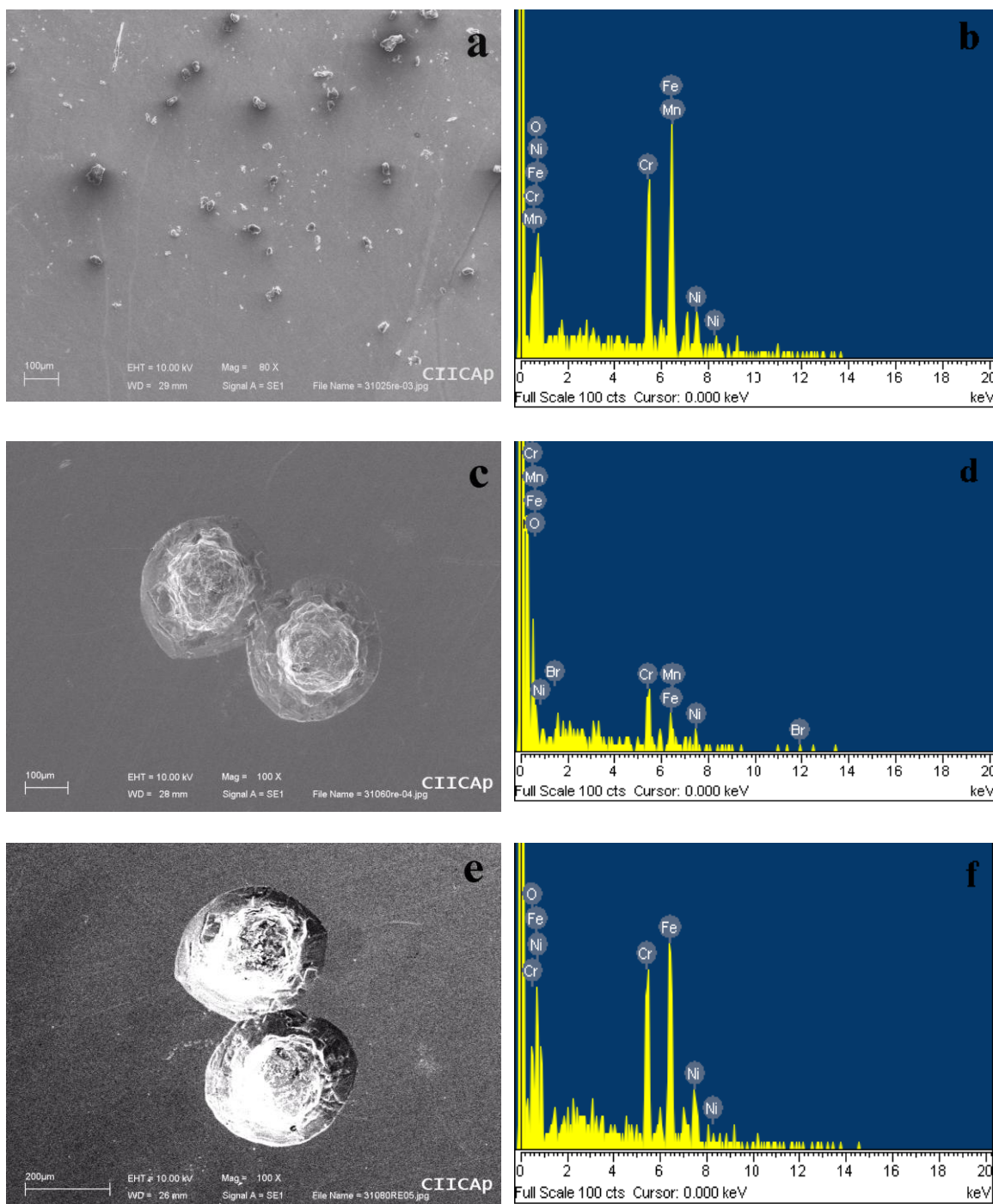


Figure 1. Micrographs of AISI-310 after exposure to the aqueous solution LiBr-H₂O, and EDX analysis of the corrosion products a,b) 25°C; c,d) 60°C; e,f) 80°C.

The amount of corrosion products seems to indicate that the material formed a protective oxide film. Pits were not observed. The EDX analysis taken from the surface of attacked sample at 25°C determined the presence of the main elements of the alloy (except silicon) and oxygen, which means that AISI-310 developed a layer of nickel, chromium, iron and manganese as a protective layer. Accordingly to the composition of the alloy and the intensity of the picks of the EDX spectrum, it seems to be that the oxide film was mainly formed of chromium and iron oxide, and in less extend of nickel and manganese. This protective layer just let the material corrode in a uniform way, not having

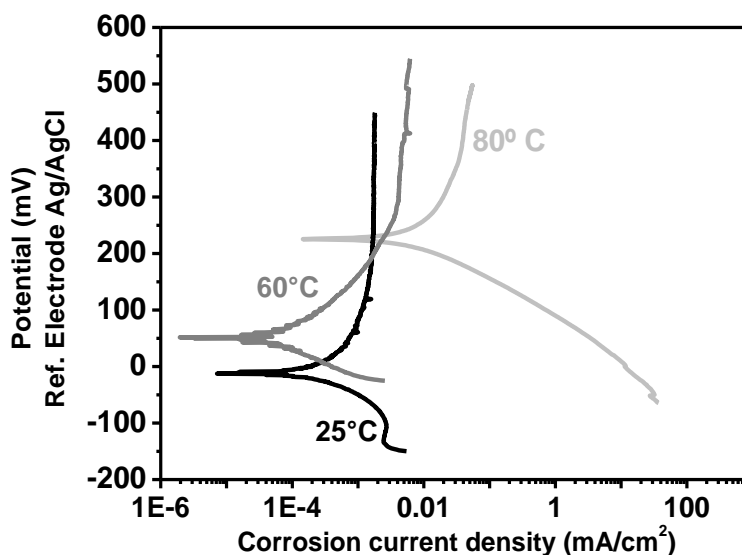
the presence of pitting or another form of corrosion attack. Figures 1.c and 1.d present a micrograph and EDX spectrum of the corroded surface exposed at 60°C, in which several pits and also a general corrosion degraded area performing as the cathodic zone are observed. The size of the pits was between 270-360 μm . According to these results, it could be said that the material suffered a mixed corrosion process. The EDX analysis shows beside the main elements of the alloy (except silicon) and oxygen, the presence of bromide, which evidences the possible formation of some bromide species, probable in the form of iron and chromium bromide. The less intensity of the main peaks of chromium and iron indicates the selective dissolution of these elements when pitting corrosion was carried out, maybe as bromides. Figure 1.d and 1.e. shows a micrograph of the corroded surface and an EDX analysis of the corrosion products formed over the metallic surface exposed at 80°C. The morphology is similar than that at 60°C, except that the size of the pits is larger, being of 310-370 μm approximately. From the SEM analysis, it is concluded that AISI-310 stainless steel is susceptible to corrode in a localized way as pitting corrosion at 60 and 80°C. At 25°C the material was more resistant, and the way in which was corroded was through a uniform process.

3.2. Polarization Curves

Figure 2 presents the polarization curves of AISI-310 at the three test temperatures. The PC's showed that the corrosion potential was nobler with temperature, being -13.0, 52.3 and 225.4 mV at 25, 60 and 80°C respectively, such as it has presented in several cases when stainless steel material is exposed in LiBr aqueous solutions [12,13]. Even though the polarization curves do not have Tafelian behavior, the extrapolation method was applied, obtaining the parameters presented in Table 1. According to these data, the higher current density corrosion was that for the higher temperature, and the smaller one was at 25°C. Some particular characteristics of each PC in their anodic branches are next: at 25°C there was a current limit of 0.002 mA/cm² in a potential range of 110.0 to 450.0 mV; this is in accord with the SEM results, since, it is expected that the corrosion rate for a type of uniform corrosion be constant and lower than that for a localized corrosion process. At 60°C, the anodic branch is alike to that at 25°C, observing that the active zone at the higher temperature is longer, changing its Tafel slope in such way that the changes of current density is very small (from 0.004 to .01 mA/cm²) with respect to the potential from 250 to 550 mV/dec. Nevertheless, the existence of a passivation region is not never evident in the range of potential for which the polarization curve was made, which would indicate the vulnerability of the material to breakdown and recovery the protective film formed by metallic oxides over the surface, which could enhance the formation of pits. At 80°C, the anodic branch was always active, observing a smaller slope with respect to 25 and 60°C, which indicates that the change in corrosion current density is a little higher. These results indicate that at 25°C, the corrosion rate would be constant and lower, such as shown in PC graphs. From the point of kinetics view, the anodic branches of the three PC's also indicate that the corrosion rate is in general expected to increase with temperature.

Table 1. Parameters of Potentiodynamic Polarization Curves of AISI-310 exposed in the corrosive solution LiBr-H₂O (50% wt.).

Parameters	25°C	60°C	80°C
ba (mV/dec)	286.4	130.0	298.5
bc (mV/dec)	97.2	49.0	67.8
E _{corr} (mV)	-13.0	52.3	225.2
I _{corr} (mA/cm ²)	4.6x10 ⁻⁴ mA/cm ²	1.4x10 ⁻⁴ mA/cm ²	5.26x10 ⁻³ mA/cm ²

**Figure 2.** Polarization curves of AISI-310 exposed to 50 (wt.%) BrLi at 25, 60 and 80°C.

3.3. Electrochemical noise measurements

Figure 3 present the current and potential time series at 25, 60 and 80°C. These records were selected for showing the major localized corrosion activity, and will be analyzed taking into account the three typical forms of electrochemical noise generated by different types of corrosion processes [8]:

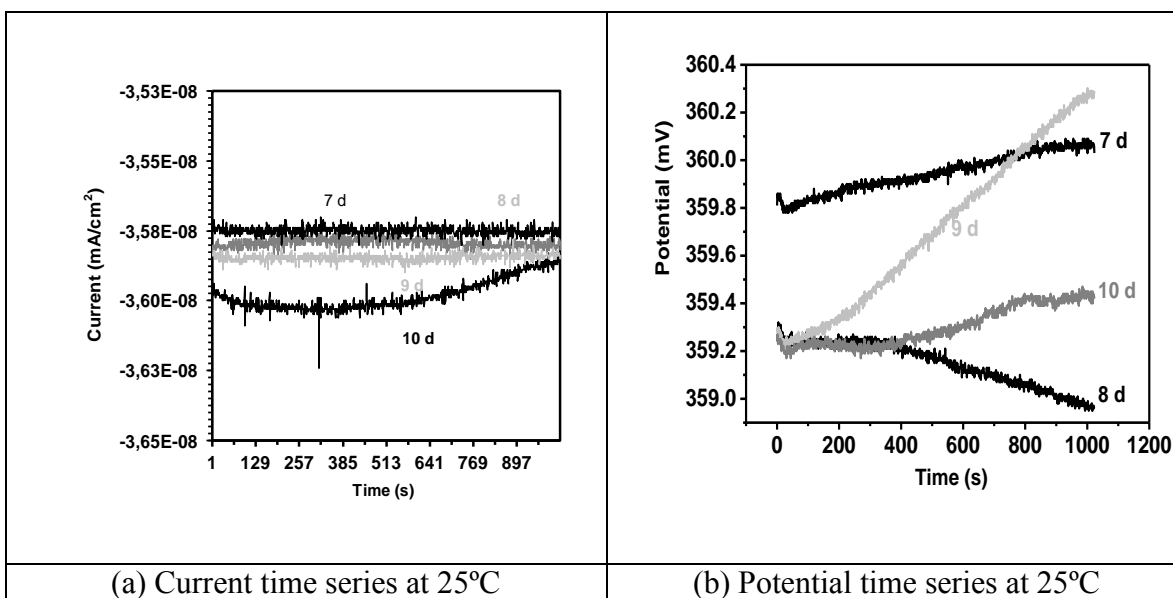
- Type I (Pitting): Consist of transients of high intensity with a high repetition rate.
- Type II (Mixed): It is a combination of transients of type I and oscillations of short amplitude.
- Type III (Uniform): the pattern noise is formed by oscillations of low amplitude.

At 25 (Fig. 3.a y 3.b) and 60°C (Fig. 3.c and 3.d) there were no important anodic or cathodic transients. The current density at 25°C presented negative and very low values, which indicates that the corrosion rate must be expected small, whereas the negative values shows the preferential dissolution of that electrode connected as the cathodic electrode, hence the direction of the current has been changed [9]. The current time series presented random oscillations of low amplitudes, not observing significant anodic transients, and only two important cathodic transients, which indicate the recovery

of the metallic oxide film. This noise pattern indicates that the material could be corroded in a uniform way, with some evidence of passivated behavior, such as was proved with SEM and the polarization curves results. With respect to the potential time series, the noise pattern is similar to the current times series, also presenting oscillations of low amplitude, being congruent with the current noise pattern.

The current time series at 60°C also show a preferential dissolution of one of the working electrodes, observing that the values of the current density are four magnitudes higher than that at 25°C, indicating an important increase in the corrosion rate with temperature. In general, at 60°C the current and potential time series showed very low intensity random oscillations similar to that obtained at 25°C, which is called white noise. This noise pattern indicates that the corrosion process would be expected in a uniform way, which is not in accord with SEM results. The potential noise was presented in a higher range, approximately 110 mV, observing to be nobler with respect to that obtained at 25°C, which is congruent with the polarization curve results, being this a particular behavior of BrLi-H₂O corrosion system with temperature [9,10].

The current and potential time series at 80°C (Fig. 3.e and 3.f) present a different noise pattern, showing major noise and an oscillatory behavior. There are more significant signals of localized corrosion or the breakdown and recovery of the passive film, especially at 5 and 6 days. In fact, the most of the time series were similar to that at the 2nd day, showing that the localized process was performed at 5th and 6th days. At the 5th and 6th days there were significant transients, observing a sudden increase in current accompanied with a sudden decrease in potential with their corresponding recovery, which, as it has been said, it can be interpreted as the rupture of the metallic oxide film or localized corrosion events [10,11]. Even though it is feasible to observe several transients at those days, it is also possible to observe random oscillations of low amplitudes, as evidence of mixed corrosion process in the rest of the time series along the experimental time [12,13]. With respect to the values of the current density, it is seen that they are smaller than that at 60°C. The results of electrochemical noise at 80°C were in agreement with SEM results, given that both techniques showed the susceptibility of AISI-310 to corrode in a localized and mixed corrosion process.



(a) Current time series at 25°C

(b) Potential time series at 25°C

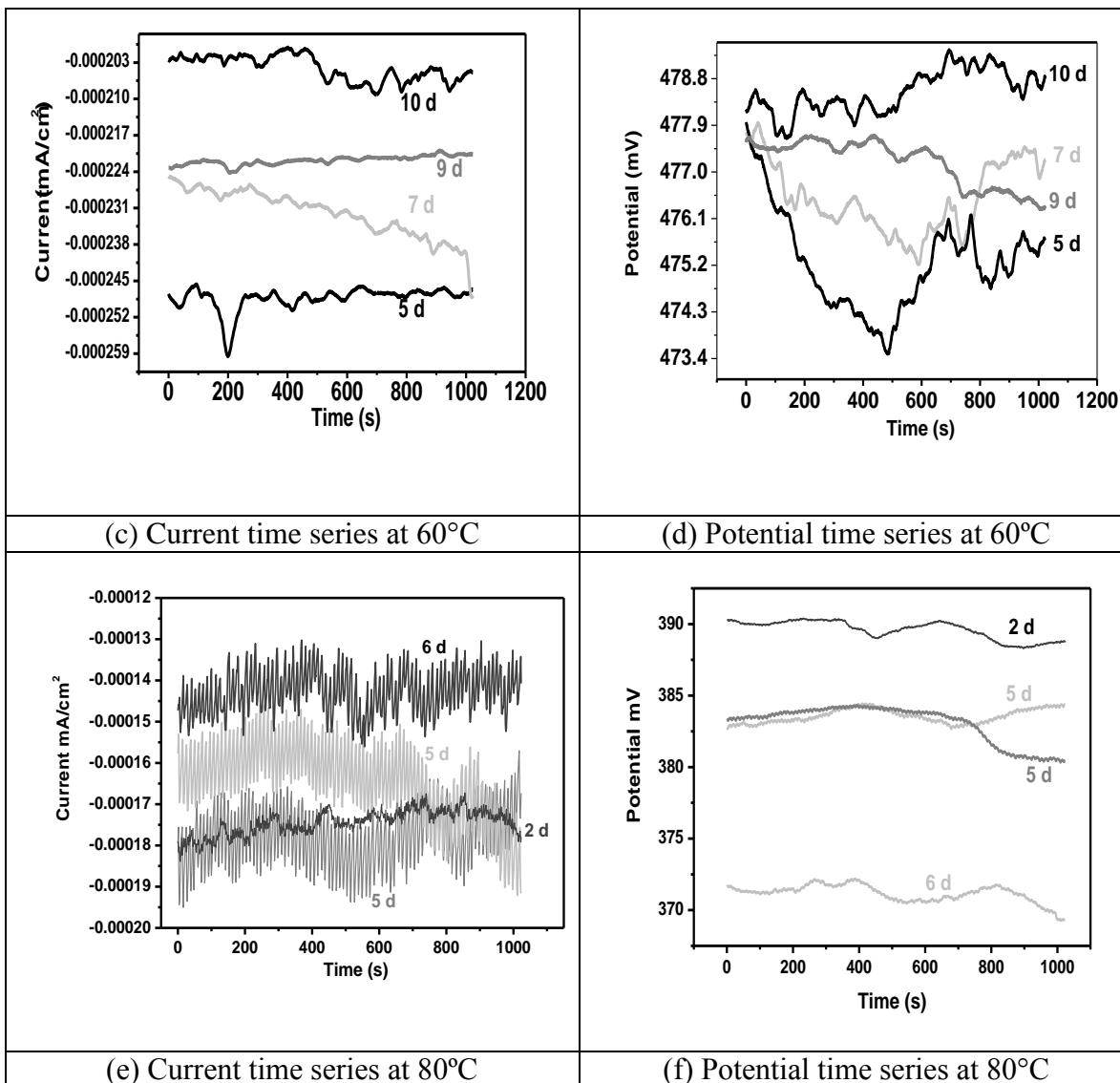


Figure 3. Current and potential time series of ASI-310 exposed to BrLi-H₂O Solution.

3.4. Localization index and corrosion rate

To corroborate the behavior of electrochemical noise signals with respect to the corrosion process, the localization index (LI) was calculated as the ratio between the current noise standard deviation σ_i over the root-mean-square current value I_{rms} [13,14], which is presented as indicator of localized corrosion activity. The analysis took into account the different ranges of LI values, which lie between 0.0 and 1.0. For current fluctuations, which are large compared to the mean current, LI will have values close to 1.0, while for current fluctuations, which are small compared to the mean current, LI will be close to 0.0 [15,16]. The values of the localization index are shown in Figure 4. LI values were calculated from every one of the time series records obtained from the electrochemical noise measurements along the experiment time.

Localization index values are mainly positioned between the mixed and uniform corrosion zones. The localization index at 25°C kept in the zone of uniform or generalized corrosion, which is in

accord with the electrochemical noise pattern and also with SEM results. At 60°C the values lie near the border between the uniform and mixed corrosion zones, whereas that at 80°C, most values lie in the zone of mixed corrosion. These results must be due to the fact that at 60°C there were no transients, while at 80°C several transients could be seen, as an indicative that the localized process was more evident at the higher temperature. At this moment, it is possible to conclude that the localization index parameter may be a complement from what current noise signals show through the electrochemical noise time series with respect to the physical evidence of corroded samples.

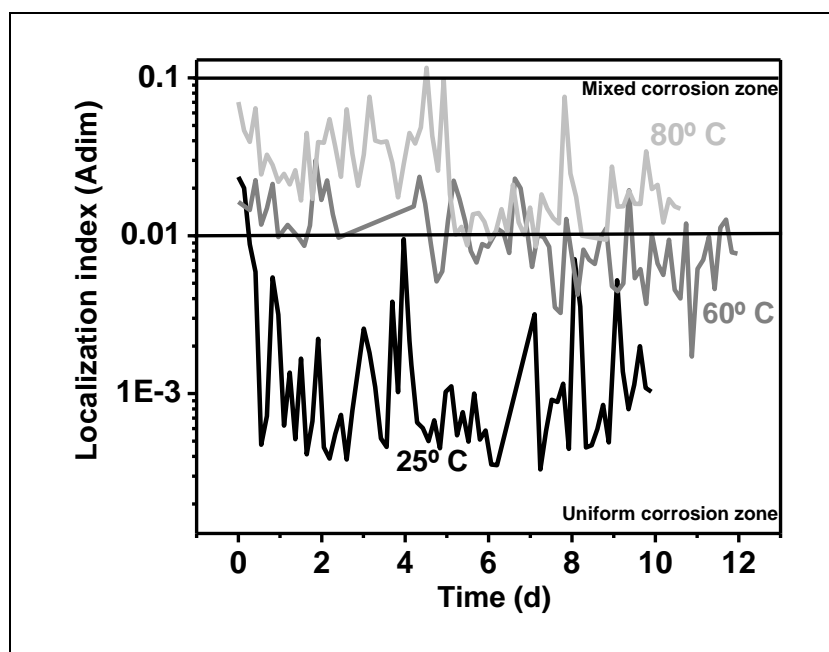


Figure 4. Localization index of AISI-310 exposed to BrLi-H₂O at different temperatures.

Fig. 5 shows the experimental corrosion rate in time obtained from the electrochemical noise data for AISI-310 stainless steel exposed to LiBr-H₂O (50.0 % wt.) at the three test temperatures. To calculate the mass loss in time, the noise resistance R_n was evaluated as the ratio of the potential noise standard deviation over the current noise standard deviation [14,15,17]. R_n data were used in the Stern-Geary equation to obtain the corrosion current density I_{corr} (mA/cm²), subsequently, the Faraday's Law [12,18,19] was utilized to obtain the mass loss, as described elsewhere [9,10]. It was necessary to obtain the Tafel slopes to calculate the Tafel constant B present in the Stern-Geary equation. Tafel slopes were determined from the experimental polarization curves at the test temperatures (see Table 1). The behavior of the corrosion kinetics at 25°C showed that the corrosion rate had an oscillatory behavior with a light tendency to increase with time, and also had the smallest values of corrosion rates, such as observed in the current times series at this temperature. This result is also in accord with the visual characterization obtained from SEM analysis, since, a uniform corrosion normally present lower corrosion rates. The corrosion kinetic at 60 and 80°C tended to diminish in time, having the highest values of corrosion rates. According to these results, the corrosion rate at 60°C presented higher values than that at 80°C, which could also be seen in the electrochemical current

noise, where the current density was higher at the smaller temperature. Also, this behavior could be due to the changes in the thermodynamic characteristics of the lithium bromide solution, because at 80°C, the aqueous solution tends to crystallize [1], therefore, the active species of bromide diminish during the corrosion process, provoking a decrease in the corrosion rate.

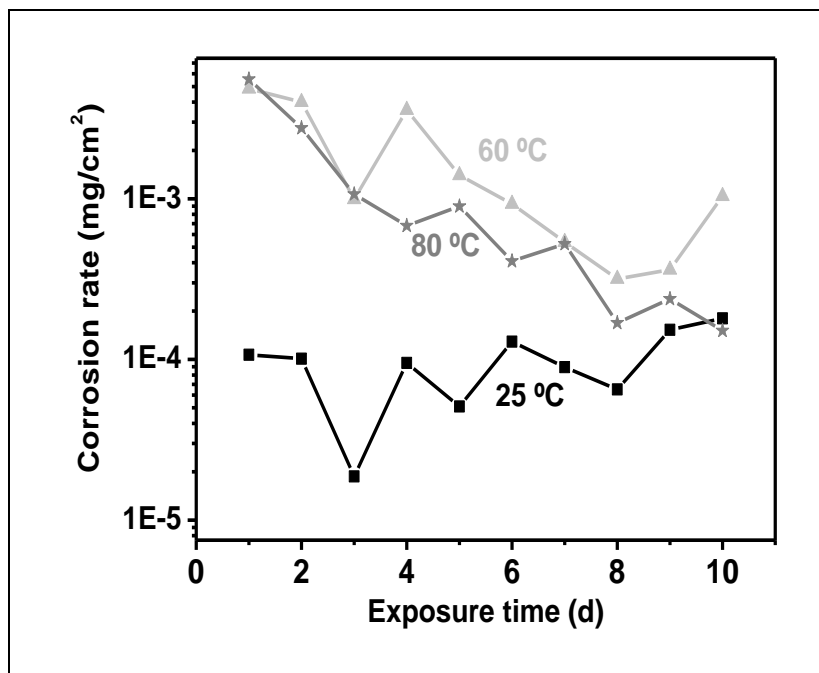


Figure 5. Corrosion rate in time obtained from the electrochemical noise data for AISI-310 stainless steel exposed to LiBr-H₂O (50.0 % wt.)

3.5. Electrochemical Impedance Spectroscopy

Figure 6 present four Nyquist and Bode diagrams of AISI-310 stainless steel during the exposure at 25°C. At the beginning and at 3h, it is observed that the Nyquist diagram tended to form semi-circles, observing that at the end of the first one, a straight line was observed, indicating the diffusion effect. Although it is not possible to determine the charge transfer resistance (R_{ct}), it seems than completing the semi-circles, the magnitude of the R_{ct} would be in an order of magnitude between 10^{+5} and 10^{+6} (very large values), which indicates that at the beginning of the corrosion process, the material was protected. At 8h, a right line with some oscillations was observed, which indicates that the corrosion process carried out by means a diffusion-controlled reaction [20]. The diffusion of species could be through the corrosive solution or through the metal-oxide film interface. The probable species diffusing in the aqueous solution could be the oxygen and bromide, whereas the possible species diffusing the interface are nickel, chromium or iron ions derivated from the oxidation reactions. At 19 hours of exposure, the formation of a semicircle was seen, which means that the corrosion mechanism changed in time. A semicircle means that an activation-controlled step was prevailing [21]. In general, could be inferred that the corrosive system at 25°C did not performance in a Tafelian way, which could be also observed in the corresponding polarization curve (See Table 1). The Tafel regions

in the polarization curves are not well defined, probably reflecting the importance of mass-transfer conditions, being the Tafel slopes very large ($b_a=286.4$ mV/dec, $b_c=97.2$ mV/dec), indicating that the diffusion of the species can have a significant influence on the rate controlling step. Tafel slopes lower than 100 mV/dec are typical for activation controlled systems, whereas Tafel slopes with larger values are typical for systems which are not purely activation or diffusion controlled [22]. In the same figure a Bode plots (Impedance vs. frequency) for the same Nyquist diagrams is presented, which shows that the impedance was not solved, being difficult to determine the charge transfer resistance. The corrosive solution resistance could be determined, being 4 ohms.cm^2 .

The Nyquist and Bode diagrams at 60°C (Figure 7) present semicircles, which indicate an activation-controlled step. This result is in accordance with the corresponding polarization curve, from which the Tafel slopes resulted much lower than that at 25°C . The Nyquist diagrams also present the values of the charge transfer resistance (R_{ct}), which is the diameter of the semicircle, observing that this variable is increasing in time, indicating that the stainless steel is protecting with time, that is why the corrosion rate is decreasing in time during the first 24 hours (see figure 5), being the resistance noise and the charge transfer resistance in agreement. In this case, the Nyquist and Bode diagrams provide the magnitudes of R_{ct} . The Bode diagrams are completely solved at the minimum frequency, being the R_{ct} as next in increasing order of time: 6762.0, 19356.0, 20017.0, 21655.0, 25801.0, 29675.0 ohms.cm^2 . The solution resistance from the Bode diagrams resulted similar to that at 25°C .

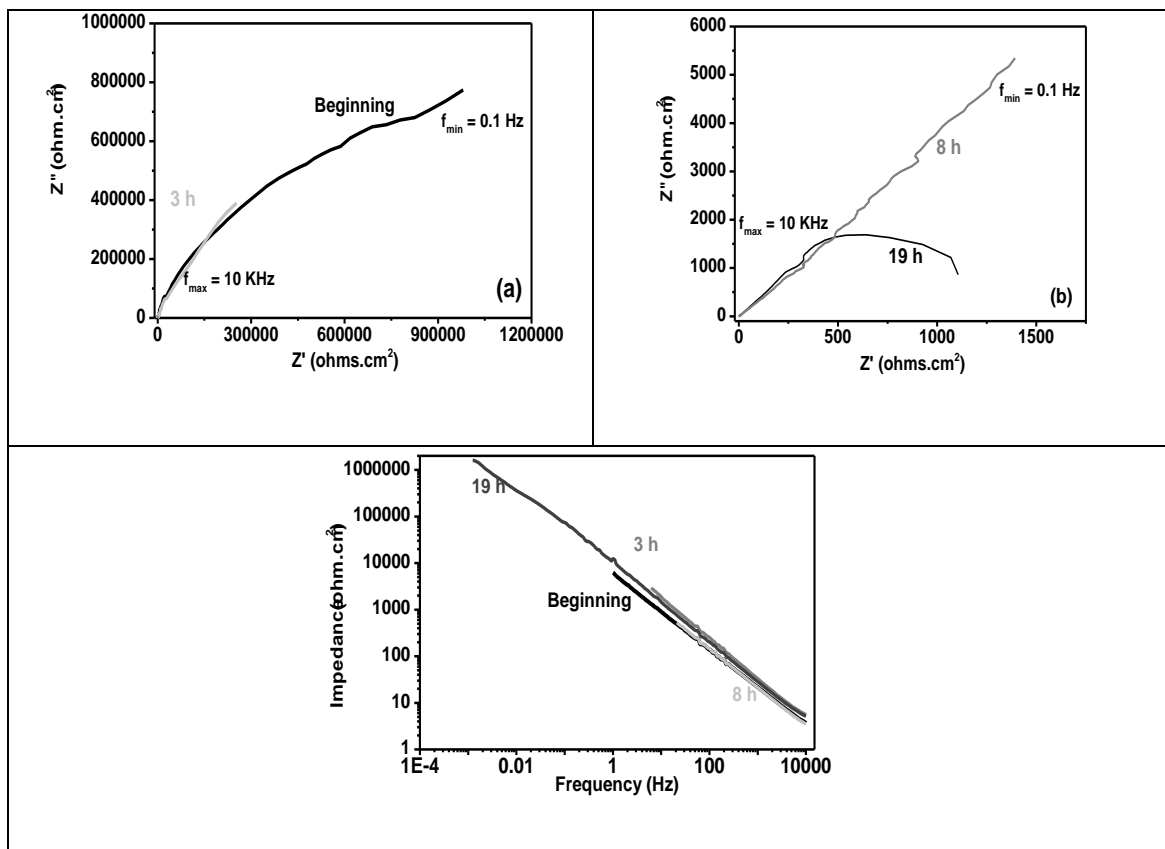


Figure 6. Nyquist and Bode diagrams of AISI-310 at exposed to BrLi-H₂O 25°C

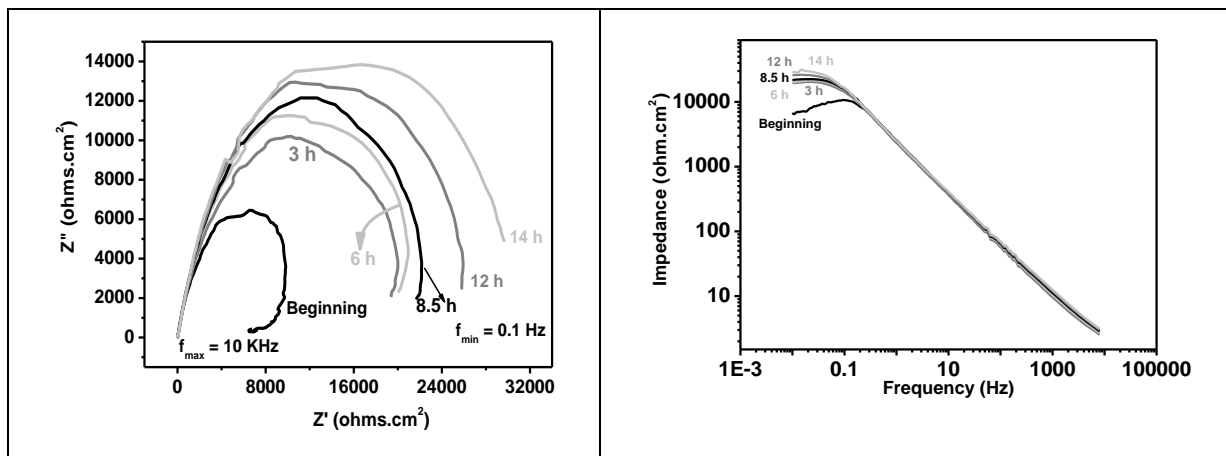


Figure 7. Nyquist and Bode diagrams of AISI-310 exposed to BrLi-H₂O at 60°C

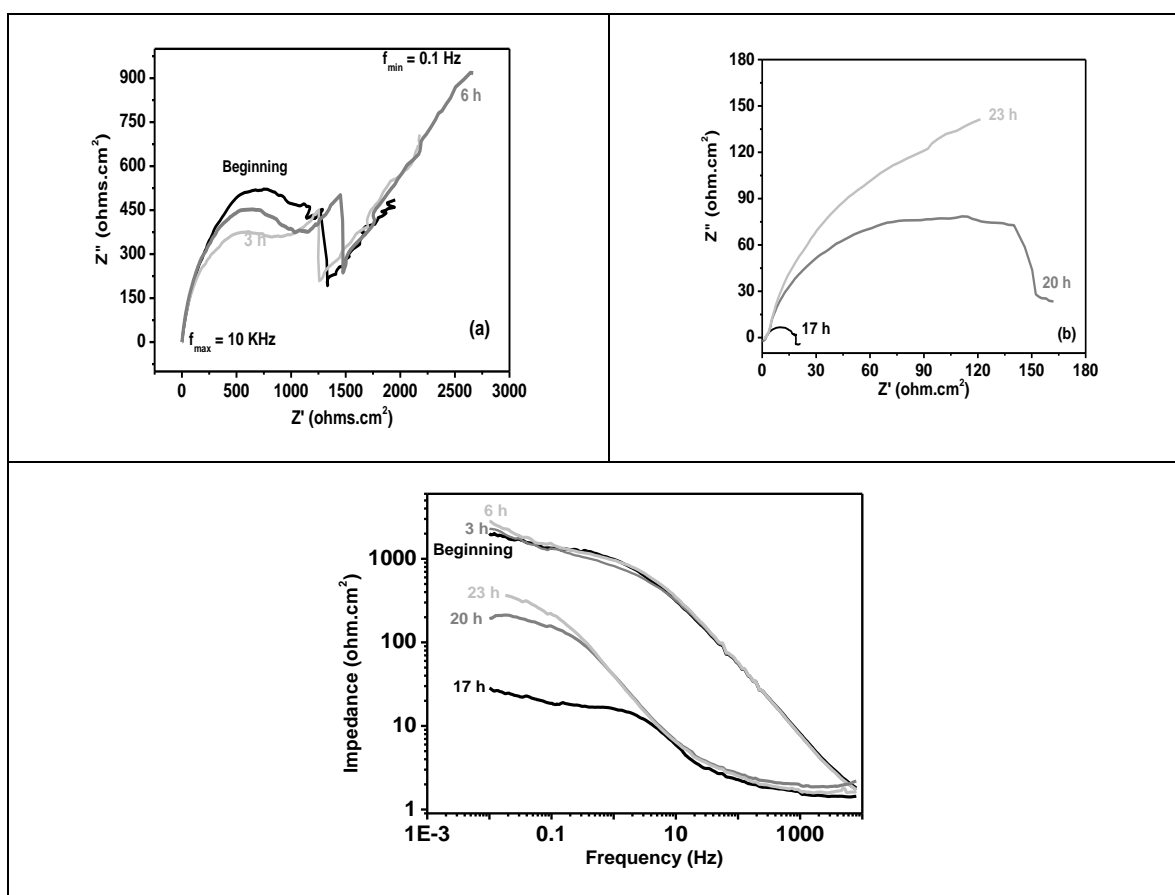


Figure 8. Nyquist and Bode diagrams of AISI-310 exposed to BrLi-H₂O at 80°C

The Nyquist diagrams at 80°C are present in Figure 8. In this case the Nyquist diagrams show that it seems to be two semicircles and then a straight line. According to the interpretation of the Nyquist diagrams [23], the two semicircles indicate the adsorption of species over the surface. The

straight line indicates the diffusion effect at this temperature until the first 6 hours. It is important to note that in these plots there are some instabilities and oscillations, which may represent the effect of the adsorption species on the surface, which are an obstacle to the diffusion or charge transfer processes. The three Nyquist plots at the last hours of the test time show semi-circles incrementing the charge transfer resistance, observing that the R_{ct} at the last hours is smaller than that at the first hours of the experimental time. The Bode plots at the same times are also presented. The impedance is solved, and it is possible to determine the R_{ct} of the six Nyquist plots. In an increasing time, the charge transfer resistances are: 2015.0, 2290.0, 2821, 29.0, 193.0, 364.0 Ohms.cm², observing in general that the corrosion rate is expected decremented in time, which is also in accordance with the first 24 hours of the corrosion rate determined through the resistance noise.

4. CONCLUSIONS

An experimental study was carried out for determining the corrosion performance of AISI-310 stainless steel exposed to LiBr-H₂O solution at 50.0 % (wt.) at 25, 60 and 80°C during 10 days. Polarization curves, electrochemical noise data, and electrochemical impedance plots were obtained experimentally, which results were supported by Scanning Electron Microscopic. From the results, the next conclusions could be stated:

Physical corrosion characterization showed that AISI-310 exposed at 25°C suffered a uniform corrosion process, whereas at 60 and 80°C a mixed corrosion process was seen.

The electrochemical noise pattern was in accord with the visual observations of the degraded surface, since at 25°C, the noise signals showed a low amplitude and high frequency pattern, while at 60 and 80°C, several medium intensity transients could be seen. The localization index parameter was a useful parameter, which was in agreement with the visual observations of the corroded samples.

The corrosion kinetics at 25°C showed that the corrosion rate had an oscillatory behavior with a light tendency to increase with time, and also had the smallest values of corrosion rates, such as observed in the current times series at this temperature, and as it was expected to be according with the physical results of the corroded samples. The corrosion kinetic at 60 and 80°C tended to diminish in time, having the highest values of corrosion rates. According to these results, the corrosion rate at 60°C presented higher values than that at 80°C, which could also be seen in the electrochemical density current noise. This behavior could be due to the changes in the thermodynamic characteristics of the lithium bromide solution, because at 80°C, the aqueous solution tends to crystallize.

With respect to the impedance results, the controlled mechanism could be determined by means the Nyquist plots, stating that at 25 and 80°C, diffusion effects are present, whereas at 60°C a charge transfer controlled mechanism was observed. These results were in agreement with the magnitudes of the Tafel slopes. These results can be explained by the fact that at 25°C, the mobility of the species is low due to the low temperature. At 80°C the LiBr aqueous solution tended to crystallize, therefore the velocity of the chemical species taking part in the corrosion process should have been slower.

ACKNOWLEDGMENTS

This work was supported by a Conacyt project granted to the first author through the number project: 52814, who thanks for this enormous support.

References

1. F. A. Holland, *Applied Thermal Eng.*, 20-9 (2000) 863.
2. R.J. Romero, M.A. Basurto-Pensado, A.H. Jiménez-Heredia, J.J. Sanchez-Mondragón, *Solar Energy*, 80 (2006) 177.
3. J. L. Guiñon, J. García-Anton, V. Pérez-Herrans, and G. Lacoste, *Corros.* 50-3 (1994) 240.
4. A. Igual-Muñoz, J. García Antón, J.L. Guiñon, and V. Pérez Herrans, *Corrosion* 59 (2003) 606.
5. E. Blasco-Tamarit, A. Igual-Muñoz, J. García-Antón, D. García-García, *Corros. Sci.*, 48 (2006) 863.
6. D. García-García, J. García-Antón, A. Igual-Muñoz, E. Blasco-Tamarit, Proc. of the European Corrosion Congress, Lisboa Portugal, *Portuguese Materials Society*, September 2005, Paper No. P-218-F
7. A. Igual Muñoz, J. García Antón, S. López Nuévalos, J. Guiñón, and V. Pérez Herranz, *Corros. Sci.*, 46 (2004) 2955.
8. C. Cuevas-Arteaga, Proceedings of the European Corrosion Congress, Lisbon Portugal, September 2005, *Portuguese Materials Society* (Ed), Paper B-13.
9. C. Cuevas-Arteaga, *Rev. Mex. de Ing. Quím.*, 5 (2006) 27.
10. C. Cuevas-Arteaga, J. Porcayo-Calderón, *Mat. Sci. & Eng. A*, 439 (2006) 435.
11. J. Castellón-Urbe, C. Cuevas-Arteaga, A. Trujillo-Estrada, *Optics and Lasers Eng.*, 46 (2008) 469.
12. C. Cuevas-Arteaga, F. Dominguez Crescencio, *Corros.*, 65 (2009) 748.
13. C. Cuevas Arteaga, M.O. Concha-Guzmán, *Corros. Eng. Sci. and Tech.*, 44-1 (2009) 57.
14. M.A. Hernandez, F. J. Rodríguez, J. Genesca, E. García, F. J. Boerio, Proceedings of NACE 56th Annual Conference, Paper No. 197 (Houston, TX: NACE, 1999).
15. C. B. Breslin, A. L. Rudd, *Corros. Sci.*, 42 (2000) 1023.
16. P.R. Roberge, R.D. Klassen, M. Tullmin, Proceedings of NACE 57th Annual Conference, Paper 281 (Houston, TX: NACE, 2000).
17. D.M. Farrell, W.M. Cox, F.H. Stott, D.A. Eden, J.L. Dawson and G.C. Wood, *High Temp. Tech.*, 3 (1985) 15.
18. J. R. Scully, in "Electrochemical, Corrosion Tests and Standards: Application and Interpretation", R. Baboian, Editor, ASTM Manual Series, American Society for Testing and Materials (ed), MNL 20, 75, Philadelphia, Pa. (1995).
19. R. Cottis, S. Turgoose, in B. C. Syrett (Ed), *Electrochemical Impedance and Noise*, NACE Corrosion Testing Made Easy (Houston, TX: NACE, 1999).
20. J. M. Sanchez-Amaya, R. A. Cottis, F. J. Botana, *Corros. Sci.*, 47 (2005) 3280.
21. F. Mansfeld, L.T. Han, C.C. Lee, C. Chen, G. Zhang and H. Xiao, *Corros. Sci.*, 39 (1997) 255.
22. F. Mansfeld, Z. Sun, E. Speckert and C. H. Hsu., Proceedings of NACE 57th Annual Conference, , Paper 418 (Houston, TX: NACE 2000).
23. A. A. Alawadhi, R. A. Cottis, Proceedings of NACE 56th Annual Conference, Paper 207 (Houston, TX: NACE 1999).